Research Report

95-02

Soft-Switched Inverter for Electric Vehicle Drives

S. Chen, T.A. Lipo

Wisconsin Power Electronics Center
University of Wisconsin-Madison
Madison WI 53706-1691

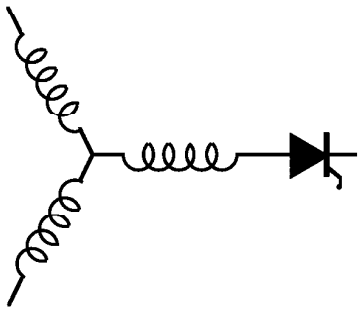

Wisconsin
Electric
Machines &
Power
Electronics
Consortium

University of Wisconsin-Madison
College of Engineering
Wisconsin Power Electronics Center
2559D Engineering Hall
1415 Johnson Drive
Madison WI 53706-1691

Soft-Switched Inverter for Electric Vehicle Drives

Shaotang Chen and Thomas A. Lipo
Department of Electrical and Computer Engineering
University of Wisconsin-Madison
1415 Johnson Drive
Madison, WI 53706-1691 USA

Abstract - **A new type of soft-switched inverter which has particular potential for battery powered applications such as electric vehicle drives is proposed. The topology is derived from the passively clamped quasi resonant link (PCQRL) circuit. By introducing magnetic coupling between the two resonant inductors, the auxiliary switches can be reduced from two to one and only a single magnetic core is required for the resonant dc link. An analysis of this novel PCQRL topology with coupled inductors is presented to reveal the various soft switching characteristics. In comparison with the conventional passively clamped continuously resonant DC Link inverter, this novel soft switched inverter can reduce voltage stresses from more than 2 p. u. to 1.1-1.3 p. u. It can also provides soft-switched PWM operation. Simulation and experiment are performed to backup the analysis.**

I. INTRODUCTION

The emergence of soft switched topologies for power conversion has brought new perspectives to high performance inverter design. In particular, the resonant dc link converters [1-4] which promise to be the next generation of industrial drives have received considerable research interest. A more recent trend seems to have evolved from continuously resonant to quasi resonant strategies owing to the various benefits regarding resonant link design and control, device rating requirements and compatibility to PWM and other conventional drive control techniques [5-12].

A new type of soft switched voltage source inverter -- the passively clamped quasi resonant link (PCQRL) inverter had been proposed in reference [13]. The PCQRL topology has the advantages of low clamp factor, simple resonance control, guaranteed zero link voltage conditions, and PWM capabilities. However, the penalties are the relatively high device count associated with the auxiliary switched inductor circuit, and the high reverse voltage requirement for the clamp diode. A solution to the drawback of large device count is the introduction of magnetic coupling between the two resonant inductors by making them share the same magnetic core as shown in Fig. 1. With magnetic coupling the current in the auxiliary inductor L_2 can reverse during the resonant transient, which makes it possible to use only one switch to control the operation of the auxiliary circuit. Thus, the device count for the auxiliary switched inductor circuit is reduced from two switches and one separate inductor to only one switch and an additional coil in the main resonant inductor.

The problem with high reverse voltage in the clamp diode can also be elegantly solved in the case of battery source operation such as in electric vehicle drives. In fact, with a battery source, the clamp diode can be connected to a low voltage battery group with a voltage equal to $(K-1)V_S$, as shown in Fig. 2a), where K is the desired link clamp factor. In this case, the turn ratio of the clamp transformer, T, can be designed to be 1:1 instead of the original 1:1/(K-1). Therefore, the maximum reverse voltage of clamp diode becomes to be only $2V_S$ instead of previous value $(1+1/(K-1))V_S$.

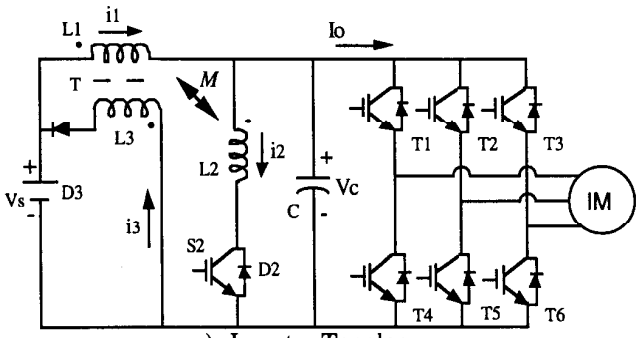

a) Inverter Topology

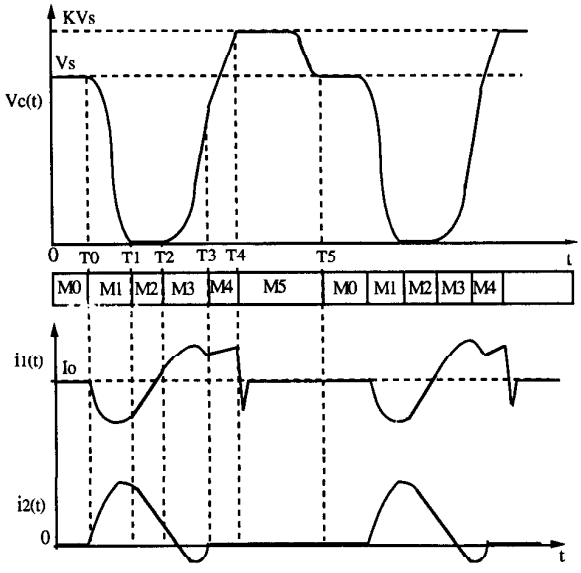

b) Resonant Link Waveforms

Fig. 1 Passively Clamped Quasi-Resonant DC Link Inverter with Coupled Inductors

Another even more simplified structure, which is also of considerable practical interest, can be derived by connecting the clamp diode directly to a separate low voltage dc source as is shown in Fig. 2b). To implement this diode clamped quasi resonant link, the low voltage dc source shown can be a separate low voltage battery in the case of electric vehicles. In the case of a diode bridge rectifier, a capacitor and a dc to dc regulator to maintain its voltage could be a practical solution as the cost and switching losses for such a low power dc to dc converter may be less than those of the passive clamp transformer.

The operation and the control requirement of the new quasi resonant inverter with coupled inductive feedback is presented in this paper. A detailed analysis of the topology is also performed to reveal the characteristics of the inverter in Section II. Simulation and experiment are performed to backup the theory. Results are discussed in Section III.

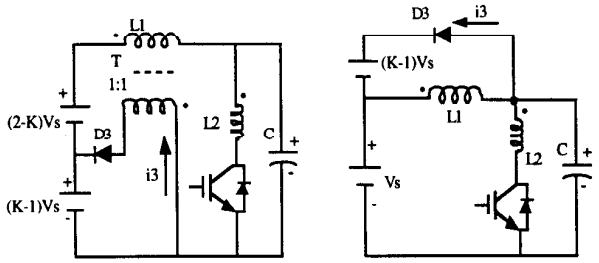

a) With 1:1 clamp transformer b) With diode clamp

Fig. 2 Different Clamps for Battery Power Sources

II. OPERATION PRINCIPLES AND ANALYSIS

The operation of the link can be explained by referring to Fig. 1. Initially, the auxiliary switch S_2 is off and the auxiliary circuit is disconnected from the inverter main power circuit. Once powered-up, the resonance between inductor L_1 and capacitor C drives the capacitor voltage up towards $2V_S$ until it is clamped at KV_S. Since the clamp factor is less than 2 p.u., the resonance between L_1 and C will limit the capacitor voltage, V_C, between $(2\text{-}K)V_S$ and KV_S which will damp towards V_S gradually due to resonant losses. Thus, the capacitor voltage will be maintained near V_S as long as the auxiliary circuit is not switched on. This state is shown in Fig. 1b) as mode 0 (M0). Assume at time T_0, a PWM switching command for the switching of the inverter poles is given. To initiate a resonant transient, the auxiliary switch S_1 is first turned on in a zero current switched manner. With S_1 on, the resonance between L_1, L_2 and C will cause the capacitor to discharge and pull down the link voltage toward a negative value. The process is called mode 1 (M1). When capacitor voltage reaches zero, the anti-parallel diodes in the inverter legs conduct and the link voltage is clamped at zero voltage condition which is shown as the mode 2 (M2). The zero voltage condition can be maintained for a short period of time determined by the link parameters. During mode 2, the inverter poles can then perform the commanded switching at zero voltage condition. In the mean time, the magnetic coupling between inductors L_1 and L_2 causes the current in the anti-parallel diodes to decrease.

Once the current in the anti-parallel diodes becomes zero, the zero voltage condition is removed, and the link resonance between L_1, L_2 and C regains control and automatically charges up the capacitor voltage. This process is indicated as mode 3 (M3). In mode 3, owing to the magnetic coupling, inductor current i_2 will reverse its direction and diode D_2 becomes conducting. The switch S_2 is then turned off in a zero voltage switching manner. Mode 3 ends when current i_2 decreases to zero and diode D_2 turns off. This result means that the auxiliary circuit is automatically disconnected from the main power circuit at the end of mode 3. In mode 4, the resonance between L_1 and C keeps driving the link voltage up to the clamp voltage KV_S. At this moment, clamp period (M5) starts to feedback excessive resonant energy to the dc source through the clamp diode D_3. After mode 5, the resonance between L1 and C will die out and the link voltage will be maintained around V_S, which is termed as pseudo steady state mode 0. The same resonant cycle will repeat if another PWM command is given.

An analysis of the link operation can be performed based on the equivalent circuits shown in Fig. 3. The main results are given as follows:

Mode 0: Pseudo steady state (S_2 off and D_2 off; D_3 off)

The link states are approximated by

$$v_c(t) = V_s \tag{1}$$

$$i_1(t) = I_o \tag{2}$$

$$i_2(t) = 0 \tag{3}$$

Mode 1: Link voltage ramps down (S_2 on and D_2 off ; D_3 off)

The resonant transient is initiated and link resonance between L_1, L_2 and C occurs. Based on the equivalent circuit in Fig. 3b, the link current and voltage can be derived as

$$v_c(t) = \frac{V_S}{L_1 + L_2 + 2M}[(L_2 + M) + (L_1 + M)\cos\omega_1(t - T_0)] \tag{4}$$

$$i_1(t) = I_o + \frac{V_S}{\omega_1(L_1 + L_2 + 2M)}[\omega_1(t - T_0) - \frac{(L_1 + M)(L_2 + M)}{L_1L_2 - M^2}\sin\omega_1(t - T_0)] \tag{5}$$

$$i_2(t) = \frac{V_S}{\omega_1(L_1 + L_2 + 2M)}[\omega_1(t - T_0) + \frac{(L_1 + M)^2}{L_1L_2 - M^2}\sin\omega_1(t - T_0)] \tag{6}$$

where

$$\omega_1 = \frac{1}{\sqrt{L_{12}C}}$$

$$L_{12} = \frac{L_1 L_2 - M^2}{L_1 + L_2 + 2M}.$$

and

$$M = k\sqrt{L_1 L_2} \qquad (k \neq 1)$$

with k being the coupling coefficient.

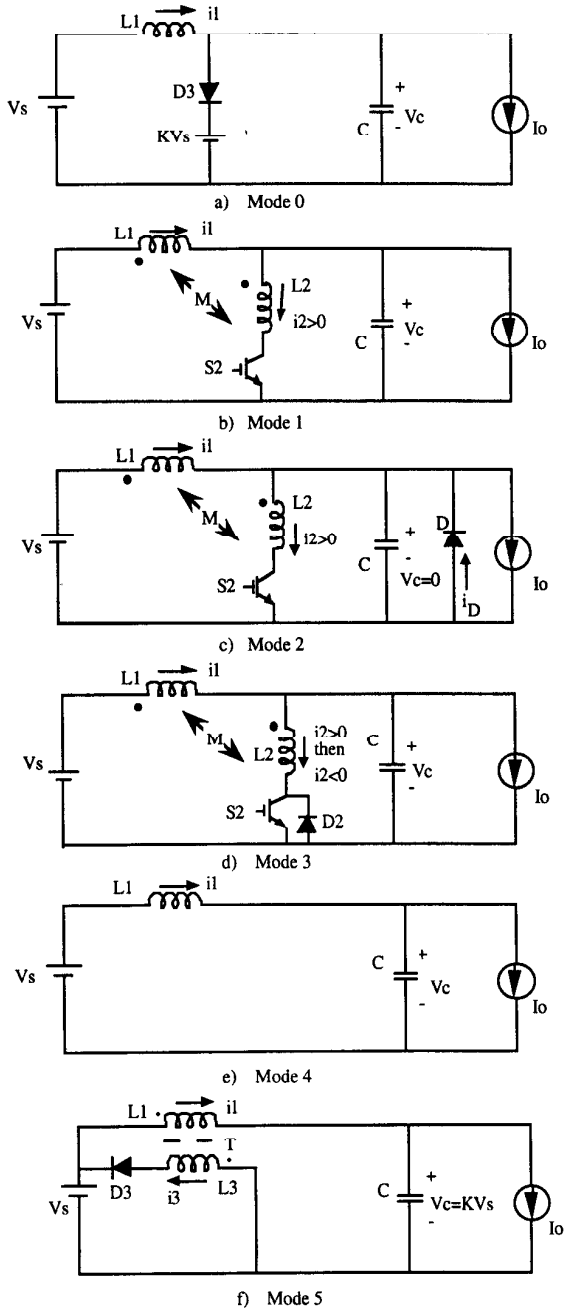

Fig. 3 Equivalent Circuit for Mode Analysis

Mode 2: Zero link voltage condition (S_2 on and D_2 off; D_3 off; Anti-parallel Diodes on)

$$v_c(t) = 0 \tag{8}$$

$$i_1(t) = i_1(T_1) + \frac{L_2 V_s}{L_1 L_2 - M^2}(t - T_1) \tag{9}$$

$$i_2(t) = i_2(T_1) - \frac{M V_s}{L_1 L_2 - M^2}(t - T_1) \tag{10}$$

The total current in the anti-parallel diodes is

$$i_d(t) = -\frac{(M + L_2)V_s}{L_1 L_2 - M^2}(t - T_1) + \frac{\sqrt{(L_1 + L_2 + 2M)(L_1 - L_2)}}{L_1 L_2 - M^2}\frac{V_s}{\omega_1} \tag{11}$$

The duration of mode 2, ΔT_2, is given by

$$\Delta T_2 = \frac{1}{\omega_1}\sqrt{\left(\frac{L_1 + M}{L_2 + M}\right)^2 - 1} \tag{12}$$

Mode 3: Link ramps up - stage 1 (S_1 on then off, and D_2 off then on; D_3 off)

Resonance caused by L1, L2 and C charges capacitor C.

$$v_c(t) = \frac{(L_2 + M)}{L_1 + L_2 + 2M} V_s[1 - \cos\omega_1(t - T_2)] \tag{13}$$

$$i_1(t) = i_1(T_2) + \frac{V_s}{\omega_1(L_1 + L_2 + 2M)}[\omega_1(t - T_2) + \frac{(L_2 + M)^2}{(L_1 L_2 - M^2)}\sin\omega_1(t - T_2)] \tag{14}$$

$$i_2(t) = i_2(T_2) + \frac{V_s}{\omega_1(L_1 + L_2 + 2M)}[\omega_1(t - T_2) - \frac{(M + L_1)(M + L_2)}{L_1 L_2 - M^2}\sin\omega_1(t - T_2)] \tag{15}$$

Note that i2(t) will become negative if a proper value of M is chosen.

Mode 4: Link ramps up - stage 2 (S_2 off and D_2 off, D_3 off)

Resonance of L_1 and C keep charging capacitor C.

$$v_c(t) = V_s - (V_s - v_c(T_3))\cos\omega_2(t - T_3) + \frac{\omega_1(L_2 + M)}{\omega_2(L_1 + L_2 + 2M)} V_s \sin\omega_1(T_3 - T_2)\sin\omega_2(t - T_3) \tag{16}$$

$$i_1(t) = I_o + \frac{V_s - V_c(T_3)}{Z}\sin\omega_2(t - T_3) + \frac{(L_2 + M)}{(L_1 + L_2 + 2M)}\frac{V_s}{Z}\sin\omega_1(T_3 - T_2)\cos\omega_2(t - T_3) \tag{17}$$

where

$$\omega_2 = \frac{1}{\sqrt{L_1 C}}$$

and

$$Z = \sqrt{\frac{L_1}{C}}$$

Mode 5: Clamp action (S_1 and S_2 off; D_3 on)

Clamp action occurs when link voltage reaches KV_S.

$$V_c(t) = KV_S \tag{18}$$

$$i_1(t) = I_o \qquad (19)$$

III. SIMULATION AND EXPERIMENTAL RESULTS

A simulation of the PCQRL topology with coupled inductors as shown in Fig. 1 has been performed to verify the operation and analysis. The resonant link parameters are chosen as L_1=28.89 μH, L_2=11.8 μH, and C=80 nF. The magnetic coupling between L1 and L2 has a coupling coefficient k=0.9, while perfect coupling between L_1 and L_3 is assumed. To realize a voltage clamp factor K=1.2, the turns ratio between inductor L1 and L3 is designed as 1:5.

For a dc bus voltage equal to 320 V, a simulation was performed to verify the analysis and to reveal the link performance at various load conditions. At t=0, the initial current in L1, i_1, and the dc link load current, I_O, are both equal to 50A. The initial capacitor voltage was set to 320 V. The auxiliary switch S_2 is turned on at t=0. The simulated link voltage and current waveforms are shown in Fig. 4. It can be observed that link voltage V_C begins to ramp down. The fall time for the link voltage is about 800 ns. The zero link voltage condition, which is utilized for soft switching of inverter poles, is maintained for about 400 ns before the link voltage automatically again rises. The rise time for the link voltage is more than 1.5 μs. It is important to mention that these waveform dv/dt parameters are very desireable for better utilization of the IGBT switching characteristics. The link voltage produces a dv/dt of about 500V/μs, a desirable value often recommended by the industry.

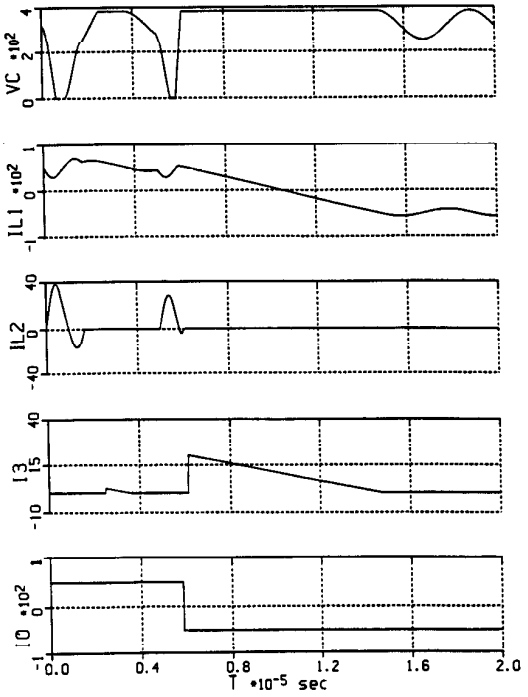

Fig. 4 Simulated Link Waveforms with DC Link Current Reversal

The worst load condition with a reversal DC link current, I_O, from positive 50 A to negative 50 A is also shown in Fig. 4. The rising edge dv/dt becomes much larger due to capacitor charge-up by the reversed link current. However, the current in auxiliary switch, i_2, is not, in fact, affected. Most of the energy is fed back through the clamp winding to the DC source. This is an advantage over the active clamp resonant link where the possibility of link inverter current reversal causes the clamp switch to be rated at a much high rating.

Due to the quasi resonant or the so called resonant transition property, all these waveforms suggest a small resonant duty cycle and small peak resonant currents. It is apparent that the resonant energy circulating inside this quasi resonant converter will be considerably smaller than the conventional continuous resonant dc link converters.

Based on the above link parameters, the novel quasi resonant inverter topology of Fig. 1 with a 320 V DC bus was constructed. The DC bus voltage was provided by a three phase rectifier in the experiment. Coaxial windings were used to build the transformer/inductors L1 and L3 for reducing leakage inductances [14]. The auxiliary switch, S_2, is turned on whenever a resonant transient is required for zero-voltage switching, while its turn-off is based on the current reversal in inductor L_2. Fig. 5 records the capacitor voltage V_C, switch S_2 gate drive input signal, and inductor L_1 and L_2 currents. The experimental measurement of link waveforms shows good agreement with simulation results. In particular, the clamp factor K achieved is seen to be well confined below 1.25 which is very close to the designed specification of 1.2.

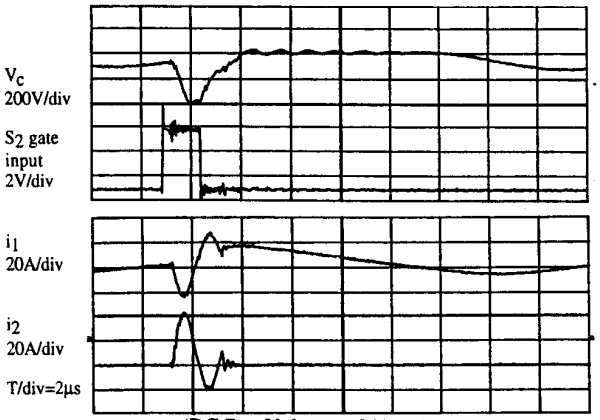

(DC Bus Voltage = 341.7 V)

Fig. 5 Measured Resonant Link Waveforms

The soft switching characteristic of the inverter can be seen from Fig. 6. which shows the resonant link voltage V_C, link zero-voltage detector output, line to line voltage and inductor L_2 current. A link zero-voltage detector circuit is used to detect the instant when capacitor voltage V_C reaches zero. The zero-voltage condition is indicated by the rising edge of the detector output. This zero voltage conditions are employed to

initiate the soft switching of the six inverter switches. The experimental measurement of the inverter output line to line voltage in Fig. 6 shows that the line to line voltage changes are clearly in synchronization with the link zero-voltage conditions. Therefore, zero turn-on losses are realized in the inverter.

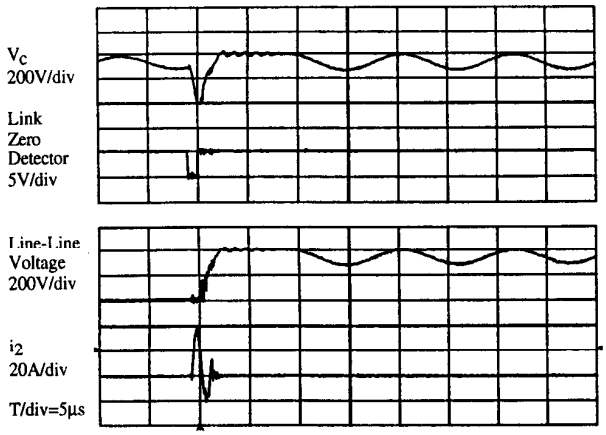

(DC Bus Voltage = 341.7 V)

Fig. 6 Zero-Voltage Switching of Inverter Switches

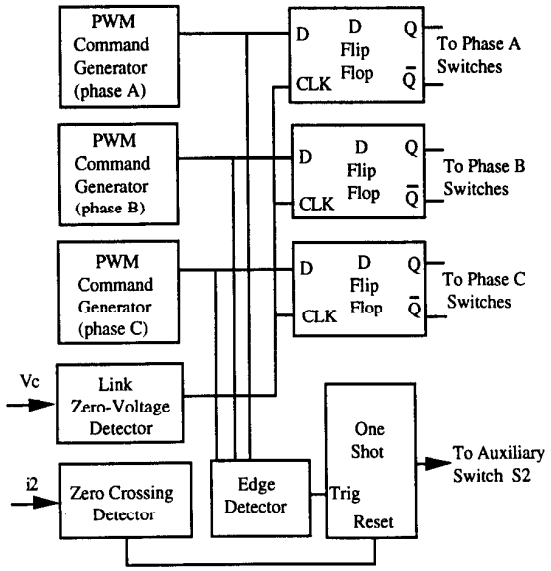

Fig. 7 Control Circuit Diagram for Soft-Switched PWM Modulation

In comparison with all other resonant link inverters, the new topology appears to provide the simplest control requirement to realize soft-switched PWM modulation. Only a minimal revision to an ordinary PWM control scheme is required. In Fig. 7, the block diagram for soft-switched PWM control of the inverter is included. The PWM command generator could be a space vector or a sine-triangle PWM. The state changes of PWM modulation commands are first detected by the edge detector which generates a turn-on signal to the auxiliary switch S_2 to initiate a resonant transient. When the link voltage reaches zero, the zero-voltage detector outputs a signal to clock-in PWM commands to the inverter switches. It synchronizes the command with the zero link instant so that the inverter only switches at zero voltage conditions. In the mean while, the zero crossing detector senses the current reversal in inductor L_2 to output a turn-off signal to switch S_2.

To demonstrate the PWM operation, a three-phase sine-triangle PWM command generator was implemented as in Fig. 7 to control the six inverter switches. The triangle carrier or the inverter switching frequency is 5 KHz. The output of the soft-switched inverter is connected directly to a three-phase, 240 V, induction motor rated at 3 HP. Fig. 8 plots the PWM modulated link waveforms when the motor is operating under zero mechanical load. The curves shows that the inverter behaves satisfactorily over all operation conditions of a typical motor-inverter drive system.

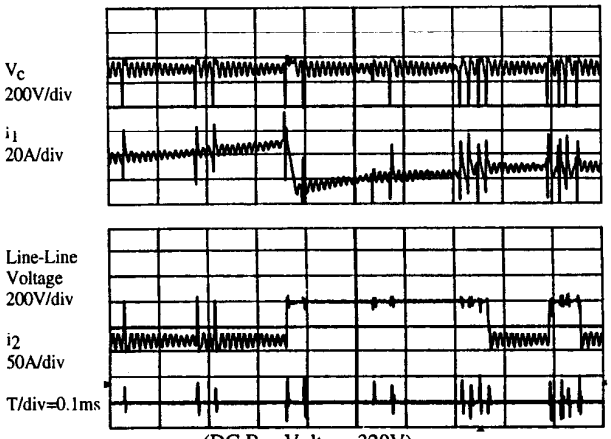

(DC Bus Voltage 320V)

Fig. 8 PWM Modulated Link Waveforms with a Motor Load

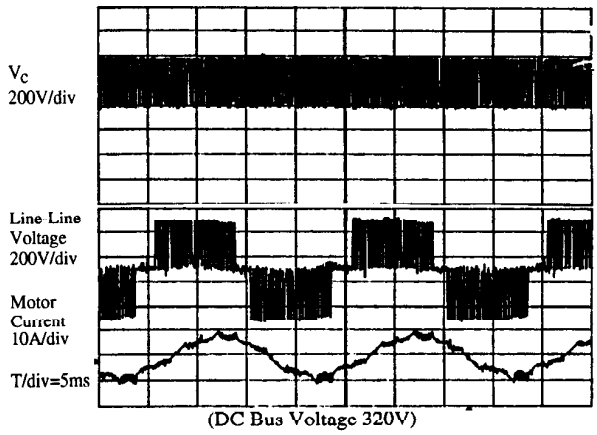

(DC Bus Voltage 320V)

Fig. 9 Motor Line to Line Voltage and Phase Current

The motor line to line voltage and phase current, together with the link voltage, are also shown in Fig. 9. It is seen that there is some distortion in the motor current. One reason for the distortion is accounted by the distortion presnet in the reference signals of the sine and triangle wavetorms of the present controller. Another

reason, however, has to be attributed to the minimum link pulse requirement in the resonant inverter. In fact, every time after S_2 is turned on and a resonant transient is initiated, it can not be turned on again in less than a certain minimum period. In the experimental design, a 10 μs minimum pulse limitation has been imposed. Due to the pulse limitation, those state changes in the PWM command which occur less than 10 μs after a previous change is made will be ignored by the control circuit. Some modification to the sine-triangle PWM is needed to prevent consecutive state changes which are less than a minimum pulse period apart. Another solution to the problem is to use space vector PWM modulation which would incorporate the minimum pulse requirement. Research on these aspects of quasi-resonant converter control is continuing.

IV. CONCLUSIONS

For battery source applications such as electric vehicle drives, the passively clamped quasi resonant dc link (PCQRL) inverter is able to provide an optimal structure for soft switching with low device ratings, simple topology, easy link implementation and control. The PCQRL topology yields the smallest device count by introducing magnetically coupled inductors in a single core. A simplification which does not require a complicated clamp transformer is also offered for practical implementation. The operation principles and link resonance control of the novel PCQRL inverter with coupled inductors are investigated. Link waveforms and operation modes are analyzed to reveal various soft switching characteristics. Successful operation of this novel PCQRL inverter with coupled inductors was demonstrated both in simulation and in an experimental implementation.

References

[1] D. M. Divan, "The Resonant DC Link Inverter - A New Concept in Static Power Conversion", IEEE-IAS Annual Conf. Rec., 1986, pp. 648-656.

[2] Y. Murai, and T. A. Lipo, "High Frequency Series Resonant DC Link Power Conversion", IEEE-IAS Annual Conf. Rec., 1988, pp. 772-779.

[3] D. M. Divan, and G. Skibinski, "Zero Switching Loss Inverters for High Power Applications", IEEE-IAS Annual Conf. Rec., 1987, pp. 627-634.

[4] A. Mertens, and D.M. Divan, "A High Frequency Resonant DC Link Inverter Using IGBTs", IPEC, Tokyo, 1990, pp. 152-160.

[5] W. McMurray, "Resonant Snubbers With Auxiliary Switches", IEEE-IAS Annual Conf. Rec., 1989, pp. 829-834.

[6] R. W. DeDoncker, and P. J. Lyons, "The Auxiliary Resonant Commutated Pole Converter", IEEE-IAS Annual Conf. Rec., 1990, pp. 1228-1235.

[7] J. He, and N. Mohan, "Parallel Resonant DC Link Circuit - A Novel Zero Switching Loss Topology With Minimum Voltage Stresses", IEEE-PESC Conf. Rec., 1989, pp. 1006-1012.

[8] J. G. Cho, H. S. Kim, and G. H. Cho, "Novel Soft Switching PWM Converter Using a New Parallel Resonant DC-Link", IEEE-PESC Conf. Rec., 1991, pp. 241-247.

[9] R. W. DeDoncker, and J. P. Lyons, "The Auxiliary Quasi-Resonant DC Link Inverter", IEEE-PESC Conf. Rec., 1991, pp. 248-253.

[10] G. Skibinski, "The Design and Implementation of a Passive Clamp Resonant DC Link Inverter for High Power Application", Ph. D. Thesis, University of Wisconsin-Madison, 1992.

[11] L. Malesani, P. Tenti, P. Tamasin, and V. Toigo, "High Efficiency Quasi Resonant DC Link Converter for Full-Range PWM", IEEE-APEC Conf. Rec., 1992, pp. 472-478.

[12] J. W. Choi, and S. K. Sul, "Resonant Link Bidirectional Power Converter Without Electrolytic Capacitor", IEEE-PESC Conf. Rec., 1993, pp. 293-299.

[13] S. Chen and T. A. Lipo "A Passively Clamped Quasi Resonant DC Link Inverter", IAS Annual Conf. Rec., 1994, Vol. 2, pp. 841-848.

[14] M. S. Rauls, D. W. Novotny and D. M. Divan, "Design Considerations for High Frequency Co-Axial Winding Power Transformers", IEEE-IAS Annual Conf. Rec., 1991, pp. 946-952.